

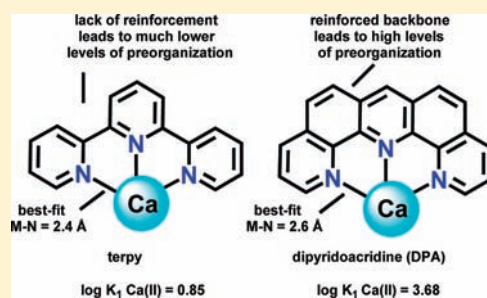
# Metal Ion Complexing Properties of Dipyridoacridine, a Highly Preorganized Tridentate Homologue of 1,10-Phenanthroline

Joanna M. Hamilton,<sup>†</sup> Jason R. Whitehead,<sup>†</sup> Neil J. Williams,<sup>†</sup> Maya El Ojaimi,<sup>‡</sup> Randolph P. Thummel,<sup>\*,‡</sup> and Robert D. Hancock<sup>\*,†</sup>

<sup>†</sup>Department of Chemistry and Biochemistry, University of North Carolina Wilmington, Wilmington, North Carolina 28403, United States

<sup>‡</sup>Department of Chemistry, University of Houston, Houston, Texas 77004, United States

**ABSTRACT:** DPA (dipyrido[4,3-*b*;5,6-*b'*]acridine) may be considered as a tridentate homologue of phen (1,10-phenanthroline). In this paper some of the metal ion complexing properties of DPA in aqueous solution are reported. Using UV–visible spectroscopy to follow the intense  $\pi$ – $\pi^*$  transitions of DPA as a function of pH gave protonation constants at ionic strength ( $\mu$ ) = 0 and 25 °C of  $\text{p}K_1 = 4.57(3)$  and  $\text{p}K_2 = 2.90(3)$ . Titration of  $10^{-5}$  M solutions of DPA with a variety of metal ions gave  $\log K_1$  values as follows: Zn(II), 7.9(1); Cd(II), 8.1(1); Pb(II), 8.3(1); La(III), 5.23(7); Gd(III), 5.7(1); Ca(II), 3.68; all at 25 °C and  $\mu = 0$ .  $\log K_1$  values at  $\mu = 0.1$  were obtained for Mg(II), 0.7(1); Sr(II), 2.20(1); Ba(II), 1.5(1). The  $\log K_1$  values show that the high level of preorganization of DPA leads to complexes 3 log units more stable than the corresponding terpyridyl complexes for large metal ions such as La(III) or Ca(II), but that for small metal ions such as Mg(II) and Zn(II) such stabilization is minimal. Molecular mechanics calculations (MM) are used to show that the best-fit M–N length for coordination with DPA is 2.60 Å, accounting for the high stability of Ca(II) or La(III) complexes of DPA, which are found to have close to this M–N bond length in their phen complexes.



## INTRODUCTION

A preorganized ligand<sup>1</sup> is one that is fixed in the conformation required to complex a target metal ion. The central fused benzo ring of phen makes it a highly preorganized ligand,<sup>2</sup> as are its substituted derivatives<sup>3,4</sup> such as PDA,<sup>5–7</sup> PDALC,<sup>8,9</sup> and DPP,<sup>10</sup> as well as macrocyclic ligands (e.g., L1 in Figure 1) where phen is incorporated as part of the macrocycle.<sup>11–13</sup> Phen complexes have been extensively studied, as evidenced by more than 4000 structures reported in the CSD<sup>14</sup> that contain phen coordinated to a metal ion. However, DPA (Figure 1), the tridentate homologue of phen, has scarcely been studied as a ligand. One would anticipate unprecedented levels of preorganization in DPA, possibly exceeding the levels found in macrocyclic ligands. Unlike macrocyclic ligands such as crown ethers,<sup>15</sup> cryptands,<sup>16</sup> and N-donor macrocycles,<sup>17</sup> DPA belongs to the class of ligands such as PDA, PDALC, and DPP, which manifest their metal ion selectivity through the presence of a highly preorganized cleft rather than a cyclic cavity. The two fused 5-membered chelate rings in tridentate complexes of DPA should<sup>2</sup> lead to a strong preference for large metal ions with an ionic radius close to 1.0 Å, which corresponds to a M–N bond length of about 2.5 Å. This preference can be understood from Scheme 1 that shows how phen-type ligands are preorganized for complexing large metal ions, while dipyridonaphthalene (DPN), which forms 6-membered chelate rings, is preorganized for complexing very small metal ions. In fact, only the very small Be<sup>2+</sup> cation could coordinate in a fairly low strain manner with

DPN, with average Be–N bond lengths to pyridyl N-donors (14 examples in the CSD<sup>14</sup>) averaging  $1.77 \pm 0.03$  Å.

Several studies of DPA complexes as catalysts,<sup>18–20</sup> as well as the synthesis of DPA and some photochemical properties of its Ru complex have been reported.<sup>20</sup> A UV–visible spectroscopic study of the metal ion complexing properties of DPA in aqueous solution, is the subject of this work.

## EXPERIMENTAL SECTION

**Materials and Methods.** DPA was synthesized by a published method.<sup>20</sup> The metal perchlorates were obtained from VWR or Strem in 99% purity or better and used as received. All solutions were made up in deionized water (Milli-Q, Waters Corp.) of  $>18$  M $\Omega$  cm<sup>–1</sup> resistivity.

**Formation Constant Studies.** Protonation constants and formation constants in aqueous solution with a variety of metal ions were determined for DPA by monitoring the intense  $\pi \rightarrow \pi^*$  transitions present in the UV spectrum. UV–visible spectra were recorded using a Varian 300 Cary 1E UV–visible Spectrophotometer controlled by Cary Win UV Scan Application version 02.00(S) software. A VWR sympHony SR601C pH meter with a VWR sympHony gel epoxy semimicro combination pH electrode was used for all pH measurements, which were made in the external titration cell, with N<sub>2</sub> bubbled through the cell to exclude CO<sub>2</sub>. The pH meter was calibrated prior to each titration, by titration of standard acid with standard base. The value of  $E^\circ$  for the cell,

Received: January 26, 2011

Published: March 17, 2011

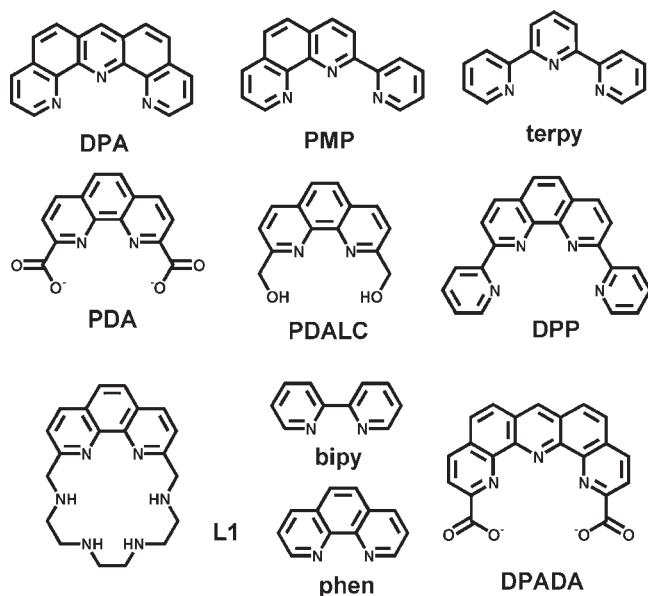
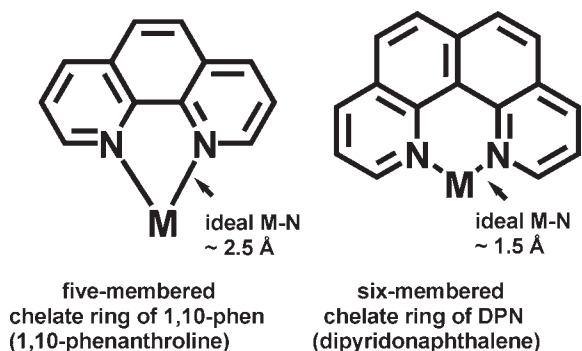


Figure 1. Ligands discussed in this paper.

### Scheme 1. Comparison of Chelating Geometries for Phen and Dipyridonaphthalene (DPN)



as well as the Nernstian slope, was obtained from a linear plot of measured values of  $E$  versus the calculated pH. The jacketed cell containing 50 mL of ligand/metal solution was thermostatted to  $25.0 \pm 0.1$  °C.

Initially, the preparation of aqueous solutions of DPA proved problematic. It was thought that DPA would be more soluble at low pH, where protonated forms should exist. Considerable effort was expended on attempts to dissolve DPA in perchloric acid solutions ranging from 10.0 to 0.01 M. The UV spectra often indicated no dissolution despite repeated heating and sonication, as indicated by the presence of only an intense (absorbance  $\geq 2.5$ ) light-scattering peak at around 220 nm. Surprisingly, it was discovered, that the neutral form of DPA was more soluble in water than the protonated forms, especially the diprotonated form. The approach finally adopted was to prepare a  $10^{-3}$  M solution of DPA in methanol, and then use this to prepare  $10^{-5}$  M aqueous solutions of DPA at neutral pH, which were stable, and did not contain light scattering peaks. The presence of 1% methanol in such solutions was considered to be insignificant.

In previous studies<sup>5–10</sup> of complexes of phen-based ligands, a peristaltic pump was used to circulate a solution of the complex through a 1.0 cm quartz flow cell situated in the spectrophotometer. It was found that, on circulating solutions of DPA complexes in this manner, the peak

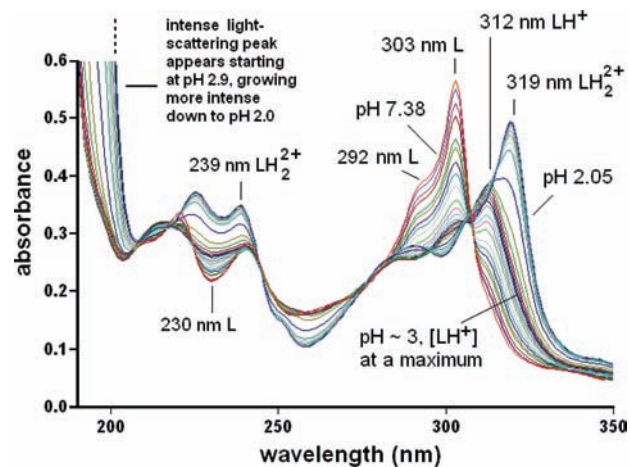
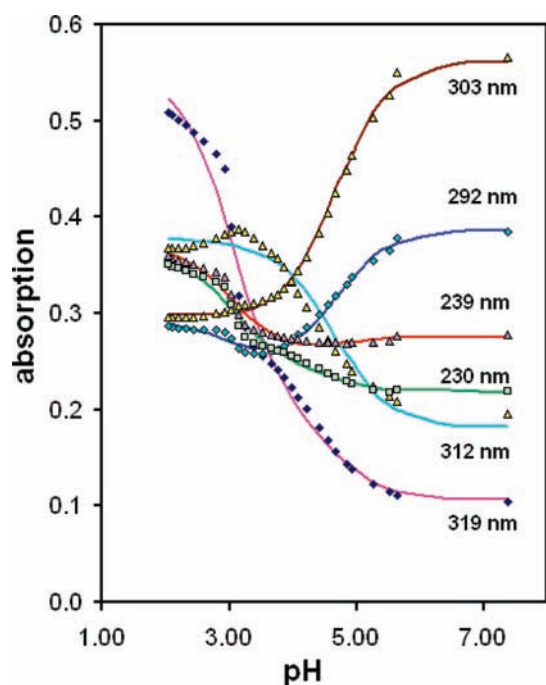


Figure 2. Spectra of  $10^{-5}$  M DPA (“L”) as a function of pH between 2.05 and 7.38. The set of spectra was generated with no electrolyte added to control ionic strength, which minimizes solubility problems. The peaks at 319 nm are assigned to diprotonated  $LH_2^{2+}$ , at 312 nm to monoprotonated  $LH^+$ , and at 303 nm to free L. Also indicated are additional wavelengths at 230, 239, and 292 nm used in calculating  $pK_1$  and  $pK_2$  in Figure 3.

intensity steadily decreased with time, suggesting that the DPA was being removed from solution, possibly by absorption into the Tygon tubing used to connect the external cell with the flow-cell in the spectrophotometer. To avoid adsorption of DPA by the tubing, the titrations were carried out in an external jacketed cell as before, but a glass Pasteur pipet was used to transfer solution to a standard 1 cm quartz cell in the spectrophotometer. The cell was not moved during the course of the titration, since movement of the cell in the spectrophotometer causes irreproducibility of the spectra.<sup>21</sup> The pH was varied in the range of 2–8 by the addition to the external titration cell of small amounts of standard molarity  $HClO_4$  or  $NaOH$  as required. After each pH adjustment, the Pasteur pipet was used to transfer a suitable quantity of the solution back and forth from the external cell to the flow cell several times to ensure adequate mixing prior to recording the spectrum. To further promote mixing, the solution in the external cell was magnetically stirred. It was also found that the addition of salts such as 0.1 M  $NaClO_4$  to control the ionic strength resulted in solubility problems with DPA. Thus the titrations were carried out with no added electrolyte, apart from the small amounts of acid or base added to adjust the pH, and the small amounts of metal ions added to complex the DPA. One thus sees in Figure 2 the series of three peaks that appear to correspond to the  $LH_2^{2+}$  (319 nm),  $LH^+$  (312 nm), and free L (303 nm). The set of spectra so obtained can be analyzed to yield two protonation constants  $pK_1 = 4.57(3)$  and  $pK_2 = 2.90(3)$ , at  $\mu = 0$ . The theoretical absorbance curves versus pH at several wavelengths were calculated using Excel.<sup>22</sup> Along with the experimental points, these curves are seen in Figure 3.

The formation constants of DPA complexes were determined by titrating an approximately neutral solution of DPA with 0.1 M solutions of the metal ion of interest, with no added electrolyte to control ionic strength. Only small total additions of these solutions were necessary to obtain sufficient metal ion concentrations to form the DPA complexes, with additions for each data point in the titration typically being 5–50  $\mu L$  at a time. The sets of spectra for the titration of  $10^{-5}$  M DPA with  $Ca(ClO_4)_2$  and  $La(ClO_4)_3$  are seen in Figures 4 and 5. For  $Zn(II)$ ,  $Cd(II)$ , and  $Pb(II)$ , the  $\log K_1$  values were too high to be determined by titration of DPA with the metal ion, and for these complexes a 1:1 solution of  $10^{-5}$  M DPA and the metal perchlorate was titrated with  $HClO_4$ . One is then determining the equilibrium quotient ( $Q$ ) for the



**Figure 3.** Variation of absorbance as a function of pH for  $10^{-5}$  M DPA for a selection of wavelengths. The solid lines are theoretical curves of absorbance versus pH calculated using Excel and protonation constants ( $pK$ ) of  $pK_1 = 4.57(3)$  and  $pK_2 = 2.90(3)$ , effectively at  $\mu = 0$ , while the points are the experimental points.

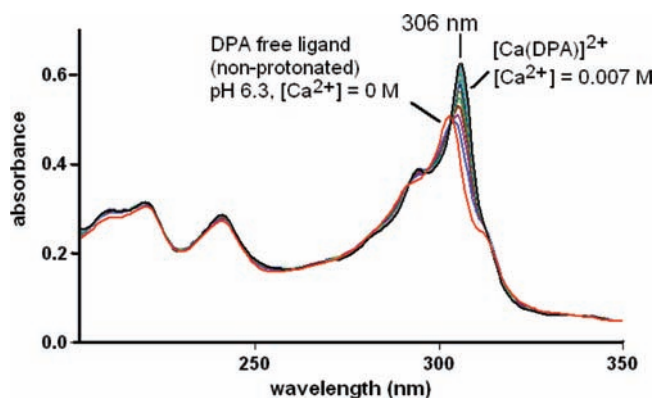


**Figure 4.** Spectra of  $10^{-5}$  M DPA in aqueous solution titrated at pH 6.3 with 0.1 M  $\text{Ca}(\text{ClO}_4)_2$  solution.

equilibrium:



The protonation constants for DPA are thus combined with  $Q$  to give  $\log K_1$  for the DPA complexes. The spectra of the DPA/Cd(II) titration are seen in Figure 6.

Theoretical absorbance curves versus metal ion concentration for the metal/DPA titrations with Mg(II), Ca(II), Sr(II), Ba(II), and La(III), or of absorbance versus pH for the  $pK$  determinations plus titrations with Zn(II) and Cd(II), were fitted to the experimental data using the SOLVER function of Excel.<sup>22</sup> The standard deviations in the  $pK$  values given in Table 1 were calculated using the SOLVSTAT macro provided with ref 22.

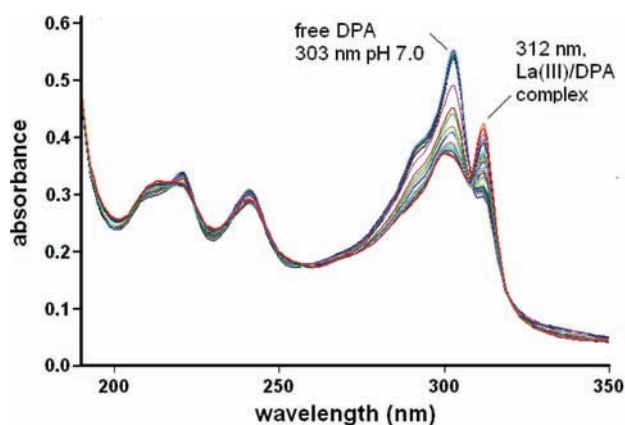


**Figure 5.** Spectra of  $10^{-5}$  M DPA in aqueous solution titrated with 0.1 M  $\text{La}(\text{ClO}_4)_3$  at pH 7.2.

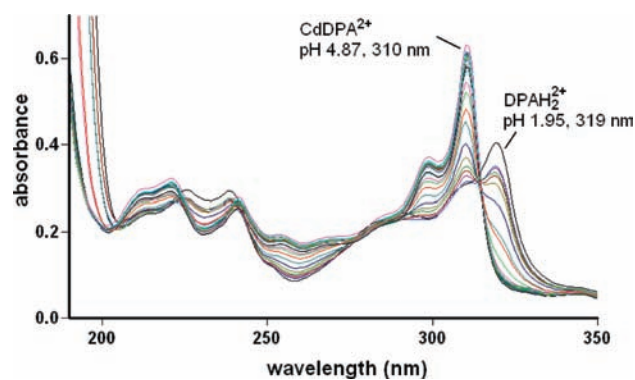


**Figure 6.** Spectra of  $10^{-5}$  M DPA plus  $10^{-5}$  M  $\text{Cd}(\text{ClO}_4)_2$  as a function of pH from pH = 4.87 to pH = 1.95. Note the increase in intensity at  $\sim 200$  nm (probably a light-scattering peak) associated with the formation of the  $\text{DPAH}_2^{2+}$  species which disappears as the Cd(II)/DPA complex forms.

**Table 1.** Formation Constants of Some Metal Ions with DPA in Aqueous Solution at 25 °C

metal ion	equilibrium	ionic strength	log $K$
$\text{H}^+$	$\text{H}^+ + \text{OH}^- \rightleftharpoons \text{H}_2\text{O}$	0	13.997 <sup>33</sup>
	$\text{H}^+ + \text{DPA} \rightleftharpoons \text{DPAH}^+$	0	4.57(3)
	$\text{DPAH}^+ + \text{H}^+ \rightleftharpoons \text{DPAH}_2^{2+}$	0	2.90(3)
$\text{Mg}^{2+}$	$\text{Mg}^{2+} + \text{DPA} \rightleftharpoons \text{Mg}(\text{DPA})^{2+}$	0.1	0.7(1)
$\text{Ca}^{2+}$	$\text{Ca}^{2+} + \text{DPA} \rightleftharpoons \text{Ca}(\text{DPA})^{2+}$	0	3.68(1)
$\text{Sr}^{2+}$	$\text{Sr}^{2+} + \text{DPA} \rightleftharpoons \text{Sr}(\text{DPA})^{2+}$	0.1	2.20(1)
$\text{Ba}^{2+}$	$\text{Ba}^{2+} + \text{DPA} \rightleftharpoons \text{Ba}(\text{DPA})^{2+}$	0.1	1.5(1)
$\text{Cd}^{2+}$	$\text{Cd}^{2+} + \text{DPA} \rightleftharpoons \text{Cd}(\text{DPA})^{2+}$	0	8.1(1)
$\text{Zn}^{2+}$	$\text{Zn}^{2+} + \text{DPA} \rightleftharpoons \text{Zn}(\text{DPA})^{2+}$	0	7.9(1)
$\text{Pb}^{2+}$	$\text{Pb}^{2+} + \text{DPA} \rightleftharpoons \text{Pb}(\text{DPA})^{2+}$	0	8.3(1)
$\text{La}^{3+}$	$\text{La}^{3+} + \text{DPA} \rightleftharpoons \text{La}(\text{DPA})^{3+}$	0	5.23(7)
$\text{Gd}^{3+}$	$\text{Gd}^{3+} + \text{DPA} \rightleftharpoons \text{Gd}(\text{DPA})^{3+}$	0	5.7(1)

## RESULTS AND DISCUSSION

**Formation Constant Determination.** The measured protonation and formation constants for DPA in aqueous solution are collected in Table 1. The solubility problems initially encountered

Table 2. Formation Constants of Some Metal Ions with DPA Compared with Those of the Less Preorganized Analogue Terpy

	metal ion								
	Mg <sup>2+</sup>	Ca <sup>2+</sup>	Sr <sup>2+</sup>	Ba <sup>2+</sup>	Zn <sup>2+</sup>	Cd <sup>2+</sup>	La <sup>3+</sup>	Gd <sup>3+</sup>	Pb <sup>2+</sup>
ionic radius (Å): <sup>a</sup>	0.74	1.00	1.19	1.36	0.74	0.96	1.03	0.94	1.19
M–N (phen) (Å): <sup>b</sup>	2.25	2.57	2.71	2.94	2.15	2.36	2.73	2.57	2.60
log K <sub>1</sub> (DPA):	0.7	3.68	2.20	1.5	7.9	8.1	5.2	5.7	8.3
log K <sub>1</sub> (terpy): <sup>c</sup>	0.74	0.85	−0.5	−0.6	7.7	6.4	2.1	2.6	6.0
Δ log K: <sup>d</sup>	~0	3.23	2.7	2.1	0.2	1.7	3.1	3.1	2.3

<sup>a</sup> Ionic radii for six-coordination, ref 33. <sup>b</sup> The average M–N lengths for the phen complexes of these ions as found in the CSD.<sup>14</sup> <sup>c</sup> Reference 34. <sup>d</sup> log K<sub>1</sub>(DPA) – log K<sub>1</sub>(terpy), which corresponds to the equilibrium M(terpy)<sup>3+</sup> + DPA ⇌ M(DPA)<sup>3+</sup> + terpy.

for DPA in aqueous solution appear to have been largely overcome by omitting the electrolyte to control the ionic strength, and avoiding tubing on which the DPA could adsorb. Figure 2 shows excellent and reproducible spectra for DPA, with clear peaks corresponding to three DPA (L) species in solution, with peaks as indicated: LH<sub>2</sub><sup>2+</sup> (319 nm), LH<sup>+</sup> (312 nm), and free L (303 nm). The protonation constants were pK<sub>1</sub> = 4.57(3) and pK<sub>2</sub> = 2.90(3), at μ = 0. It should be emphasized that the titration began at pH 7.38 with no added electrolyte, and that acid was added to lower the pH, so that in the region where the equilibria corresponding to pK<sub>1</sub> and pK<sub>2</sub> were being monitored, the electrolyte (HClO<sub>4</sub>) concentration did not exceed 10<sup>−3</sup> M, so one is justified in regarding the ionic strength as being effectively zero. The fit of the theoretical absorption curves versus pH in Figure 3 to the experimental data is quite good. Toward the end of the titration, as one approached pH 2.0, a light scattering peak began to appear, corresponding to insolubility of the LH<sub>2</sub><sup>2+</sup> species. This effect can be discerned in Figure 3 where some erratic behavior of the experimental absorption points can be seen in the absorbances at 312 nm. This effect may somewhat affect the determination of pK<sub>2</sub>, which may not be as accurate as suggested by the data fitting using SOLVER in Excel. The insolubility of the LH<sub>2</sub><sup>2+</sup> species helps to explain the inability to prepare solutions of DPA in HClO<sub>4</sub>. This insolubility probably derives from stabilization of the solid salts of the LH<sub>2</sub><sup>2+</sup> species by π-stacking.<sup>23,24</sup> One finds for phen that the neutral ligand in the solid state is not π-stacked,<sup>25</sup> but packs edge-on, with H-atoms from one phen interacting at right angles to the π-system of an adjacent phen. For face-to-face π-stacking, the π-system of at least one area of a molecule such as phen has to be rendered electron-poor,<sup>23,24</sup> most commonly by protonation, to interact with the electron-rich portion of a second phen, as seen for the monoprotonated phenH<sup>+</sup> cation.<sup>26</sup>

The metal ion formation constants for complexes of Mg(II), Ca(II), Sr(II), Ba(II), and La(III) were determined by titrating a 10<sup>−5</sup> M DPA solution with a metal ion solution at pH ~ 7.0. This direct method means that the determined log K<sub>1</sub> values for these metal ions are not dependent on the protonation constants of DPA determined above. For Cd(II), Zn(II), and Pb(II), the log K<sub>1</sub> values with DPA in Table 1 are reported with standard deviations of 0.1 because of the involvement of a slightly uncertain value of pK<sub>2</sub> for DPA in the calculation of these log K<sub>1</sub> values.

As has been found with phen coordination,<sup>27</sup> complex formation does not markedly affect the π–π\* transitions of the free ligand. The sharp peak at 303 nm in the free ligand shifts to 306 nm in the Ca(II) complex, 311 nm in the Zn(II) complex, and 312 nm in the La(III) complex. These shifts appear to

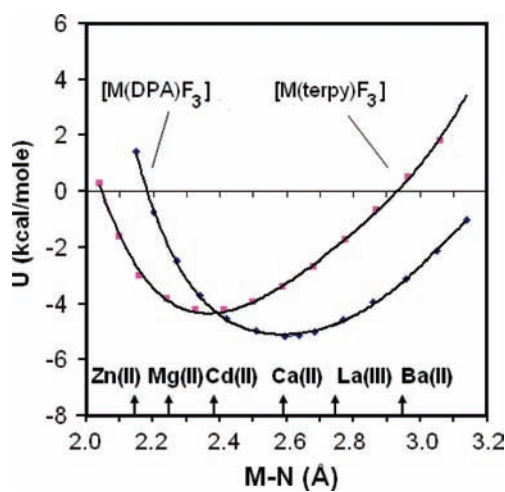
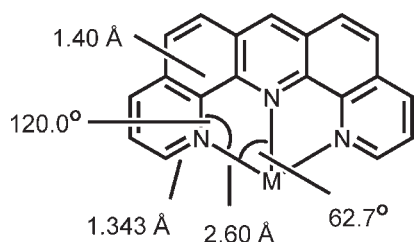


Figure 7. Variation of strain energy ( $U$ ) calculated by molecular mechanics for the complexes  $[M(\text{DPA})\text{F}_3]$  and  $[M(\text{terpy})\text{F}_3]$  as a function of ideal M–N length from 2.0 to 3.2 Å. The minimum in the curve indicates that the metal ion that would coordinate with DPA with the least strain would have a M–N length of 2.60 Å, and with terpy a M–N length of 2.41 Å. The arrows indicate the mean M–N lengths for phen complexes of the metal ions indicated, obtained from the CSD.<sup>14</sup>

correlate with how strongly one might expect the complexed metal ion to interact with the π-system of DPA. One notes that, on protonation, the same sharp peak shifts to 312 nm in the monoprotonated form of the ligand and to 319 nm in the diprotonated form.

The effect of the high levels of preorganization on the thermodynamic stability of complexes of DPA relative to those of its less preorganized analogue terpy (2,2',6,2''-terpyridine) is seen in Table 2. The table contains ions that may be described as large, that is, with ionic radii ( $r^+$ ) between 1.0 and 1.2 Å, medium with  $0.8 < r^+ < 1.0$  Å, and small, with  $r^+ < 0.8$  Å. Metal ions with  $r^+ > 1.2$  Å are regarded as very large. One sees that for large metal ions, the DPA complexes are stabilized relative to the terpy analogues by some three log units in log K<sub>1</sub>. This is typical for stabilizations attributed to the macrocyclic or cryptate effect.<sup>2</sup> For small metal ions such as Zn(II) and Mg(II), the stabilization of the DPA complexes relative to the terpy complexes is negligible. As commented by a reviewer, the very large Ba<sup>2+</sup> ion experiences a somewhat smaller stabilization of its DPA complex relative to its terpy complex. One can use MM (molecular mechanics) calculations to determine<sup>28,29</sup> the ideal M–N bond length for coordination with DPA. One calculates the strain energy ( $U$ ) of the complex as a function of M–N bond lengths, and the minimum energy of the curve indicates the best-fit M–N length for ligand

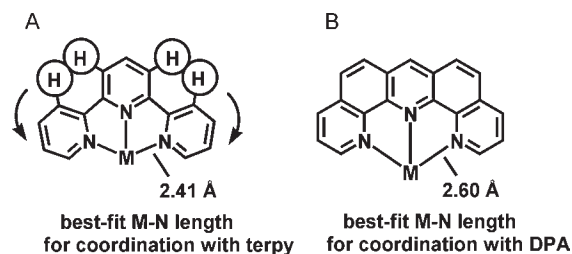
Scheme 2. Ideal Geometry for Coordination with DPA



coordination. Such calculations were carried out with HyperChem,<sup>30</sup> which allows for adjustment of MM parameters, in this case the strain-free M–N bond length. The calculations were carried out for the complexes  $[M(\text{DPA})\text{F}_3]$  and  $[M(\text{terpy})\text{F}_3]$ , where the force constant for bond length deformation of the M–N bond is set to  $0.7 \text{ mdyne } \text{Å}^{-1}$ , which has been found to be a satisfactory value for such calculations.<sup>28,29</sup> The MM force field used in HyperChem was the MM+ force field, which is essentially the MM2 force field of Allinger.<sup>31</sup> Figure 7 shows the change in  $U$  versus M–N bond length for the DPA and terpy complexes, which indicates that the minimum strain energy occurs with M–N bond lengths of  $2.60 \text{ Å}$  for a DPA complex, and  $2.41 \text{ Å}$  for a terpy complex. In generating these curves, experimentation showed that the minimum strain M–N bond length was rather sensitive to the detailed geometry of the pyridyl rings of DPA and terpy. In particular, the ideal C(ar)–N(ar) (ar = aromatic) bond lengths of  $1.26 \text{ Å}$  used in the MM+ force field for aromatic pyridine rings produced geometries that did not agree with those of phen or terpy complexes in the CSD. The C(ar)–N(ar) bond lengths in phen complexes (from 12,600 distinct C(ar)–N(ar) bonds in  $\sim 4000$  structures in the CSD) averaged  $1.343(3) \text{ Å}$ , and this value was used as the ideal C(ar)–N(ar) bond length in the calculations. The minimum strain structure for coordination within the cleft of DPA is as indicated in Scheme 2:

The average M–N lengths obtained from the CSD<sup>14</sup> for phen complexes of some metal ions of interest are indicated in Table 2 and in Figure 7: Mg(II),  $2.25(4) \text{ Å}$  (11 examples); Ca(II),  $2.57(4) \text{ Å}$  (17 examples); Sr(II),  $2.71(5) \text{ Å}$  (11 examples); Ba(II),  $2.94(6) \text{ Å}$  (18 examples); Zn(II),  $2.15(5) \text{ Å}$  (318 examples); Cd(II),  $2.36(4) \text{ Å}$  (268 examples); Gd(III),  $2.57(3) \text{ Å}$  (21 examples); La(III),  $2.73(3) \text{ Å}$  (60 examples); Pb(II)  $2.60(11) \text{ Å}$  (91 examples). Figure 7 shows that, from a consideration of M–N lengths, metal ions such as Zn(II) and Mg(II) do not fit DPA well, where the best-fit M–N length is  $2.60 \text{ Å}$ . Thus there is in Table 2 little stabilization of the DPA complexes of Mg(II) and Zn(II) relative to the terpy complexes.<sup>32,34</sup> On the other hand, Ca(II), Gd(III), or La(III) are much nearer to the ideal size for coordination with DPA, and so show large stabilizations of the DPA complex relative to the terpy complex (Table 2). It had been expected that, because of its greater rigidity, the  $U$  versus M–N curve for the DPA complex would be much steeper than the curve for the terpy complex. However, the difference in shape between the two curves is not marked. Rather, the minimum in the terpy curve occurs at a shorter M–N bond length than for the DPA complexes. The greater stabilization for the DPA complexes of large metal ions thus reflects the fact that the best-fit metal ion for coordination with DPA at  $2.60 \text{ Å}$  is larger than the best-fit size for coordination with terpy at  $2.41 \text{ Å}$ . Small metal ions

Scheme 3. (A) van der Waals Repulsion between H Atoms Forces Outer Pyridines Towards Each Other, Decreasing Best-Fit M–N Length; (B) No Steric Backbone Crowding on DPA



such as Zn(II) and Mg(II) do comparatively well with terpy because it fits better with small metal ions. The preference of terpy for smaller metal ions appears to arise from nonbonded repulsions between the H-atoms on C3 and C3', and C5' and C3'' of terpy. In a planar conformation these repulsions tend to push the two outermost pyridines toward one another leading to decreased M–N bond lengths (Scheme 3). These repulsions could also be partially avoided by twisting around the interpyridine bond which would distort the metal coordination and weaken the M–N bonding.

As indicated by a reviewer, the somewhat smaller increase in  $\log K_1$  ( $2.3 \log$  units) for the DPA relative to the terpy complex of Pb(II) is a little surprising in relation to the closeness of the average M–N bond lengths of the Pb(II) phen complexes to the ideal M–N length of  $2.60 \text{ Å}$  for coordinating in the cleft of DPA. The occurrence of a stereochemically active lone pair on Pb(II) complexes<sup>35,36</sup> can affect the Pb–N lengths depending upon the orientation of the donor atoms of the ligand relative to the lone pair, and the degree of distortion of the coordination geometry of the Pb(II) induced by the lone pair. In particular, the presence of other covalently bound donor atoms such as other N or S-donors can displace the phen from the favored coordination site opposite the lone pair, and lengthen the Pb–N bonds. In some examples, with no competing covalently bound donor atoms, the Pb–N bonds in the phen complex can be as short<sup>37</sup> as  $2.47 \text{ Å}$ , which might be a better indication of the optimal Pb–N bond lengths in phen complexes of Pb(II).

## CONCLUSIONS

The reinforced backbone of DPA stabilizes complexes of larger metal ions such as Ca(II), Gd(III), or La(III), with an increase of some 3 log units in  $\log K_1$  compared to its less preorganized analogue terpy. The rigid cleft of DPA forms two five-membered chelate rings which favor larger metal ions<sup>2</sup> and shows minimal stabilization relative to terpy with smaller metal ions, such as Zn(II) and Mg(II). Metal ions such as Ba(II) that are too large for the cleft of DPA also show smaller stabilizations relative to the terpy complex. MM calculations suggest that the best-fit size of a metal ion for coordination with DPA should have M–N bond lengths of  $2.60 \text{ Å}$ . Because of the high thermodynamic stability of the complexes DPA forms, ligands such as DPA may be of interest in such applications as separating Am(III) from Lanthanide(III) ions in reprocessing of spent nuclear fuel.<sup>38,39</sup> The neutral ligand DPA is moderately soluble in water ( $10^{-5} \text{ M}$ ), compared to phen which is soluble up to about  $10^{-3} \text{ M}$ , but DPA is much less soluble below pH 3.0, where the protonated forms in the solid state may be

stabilized by  $\pi$ -stacking. DPA is also much less soluble in the presence of inert electrolytes such as NaCl or NaClO<sub>4</sub>, which “salt” it out.

## AUTHOR INFORMATION

### Corresponding Author

\*E-mail: thummel@uh.edu (R.P.T.), hancockr@uncw.edu (R.D.H.).

## ACKNOWLEDGMENT

J.M.H., J.R.W., N.J.W., and R.D.H. thank the University of North Carolina Wilmington and the Department of Energy (Grant DE-FG07-07ID14896) for generous support of this work. R.P.T. and M.E.O. thank the Robert A. Welch Foundation (E-621) and the National Science Foundation (CHE-0714751) for support.

## REFERENCES

- (1) Cram, D. J.; Cram, J. M. *Acc. Chem. Res.* **1978**, *11*, 8.
- (2) Hancock, R. D.; Martell, A. E. *Chem. Rev.* **1989**, *89*, 1875.
- (3) Hancock, R. D.; Melton, D. L.; Harrington, J. M.; McDonald, F. C.; Gephart, R. T.; Boone, L. L.; Jones, S. B.; Dean, N. E.; Whitehead, J. R.; Cockrell, G. M. *Coord. Chem. Rev.* **2007**, *251*, 1678.
- (4) Bencini, A.; Lippolis, V. *Coord. Chem. Rev.* **2010**, *254*, 2096.
- (5) Melton, D. L.; VanDerveer, D. G.; Hancock, R. D. *Inorg. Chem.* **2006**, *45*, 9306.
- (6) Dean, N. E.; Hancock, R. D.; Cahill, C. L.; Frisch, M. *Inorg. Chem.* **2008**, *47*, 2000.
- (7) Williams, N. J.; Dean, N. E.; VanDerveer, D. G.; Luckay, R. C.; Hancock, R. D. *Inorg. Chem.* **2009**, *48*, 7853.
- (8) Gephart, R. T.; Williams, N. J.; Reibenspies, J. H.; De Sousa, A. S.; Hancock, R. D. *Inorg. Chem.* **2008**, *47*, 10342.
- (9) Gephart, R. T.; Williams, N. J.; Reibenspies, J. H.; De Sousa, A. S.; Hancock, R. D. *Inorg. Chem.* **2009**, *48*, 8201.
- (10) Cockrell, G. M.; Zhang, G.; VanDerveer, D. G.; Thummel, R. P.; Hancock, R. D. *J. Am. Chem. Soc.* **2008**, *130*, 1420.
- (11) Bencini, A.; Berni, E.; Bianchi, A.; Fornasari, P.; Giorgi, C.; Lima, J. C.; Lodeiro, C.; Melo, M. J.; Seixas de Melo, J.; Parola, A. J.; Pina, F.; Pina, J.; Valtancoli, B. *Dalton Trans.* **2004**, 2180.
- (12) Bazzicalupi, C.; Bencini, A.; Fusi, V.; Giorgi, C.; Paoletti, P.; Valtancoli, B. *J. Chem. Soc., Dalton Trans.* **1999**, 393.
- (13) Bazzicalupi, C.; Bencini, A.; Bianchi, A.; Giorgi, C.; Fusi, V.; Valtancoli, B.; Bernado, M. A.; Pina, F. *Inorg. Chem.* **1999**, *38*, 3806.
- (14) Cambridge Crystallographic Data Centre, 12 Union Road, Cambridge CB2 1EZ, United Kingdom (2009).
- (15) Pederson, C. J. *J. Am. Chem. Soc.* **1967**, *89* (2495), 7017.
- (16) Lehn, J. M. *Acc. Chem. Res.* **1978**, *11*, 49.
- (17) Cabbiness, D. K.; Margerum, D. W. *J. Am. Chem. Soc.* **1969**, *91*, 6540.
- (18) Chen, H.; Tagore, R.; Das, S.; Incarvito, C.; Faller, J. W.; Crabtree, R. H.; Brudvig, G. W. *Inorg. Chem.* **2005**, *44*, 7661.
- (19) Groen, J. H.; De Zwart, A.; Vlaar, M. J. M.; Ernsting, J. M.; Van Leeuwen, P. W. N. M.; Vrieze, K.; Kooijman, H.; Smeets, W. J. J.; Spek, A. L.; Budzelaar, P. H. M.; Xiang, Q.; Thummel, R. P. *Eur. J. Inorg. Chem.* **1998**, *8*, 1129.
- (20) Hung, C.-Y.; Wang, T.-L.; Jang, Y.; Kim, W. Y.; Schmehl, R. H.; Thummel, R. P. *Inorg. Chem.* **1996**, *35*, 5953.
- (21) Skoog, D. A.; Holler, E. J.; Crouch, S. R. *Principles of Instrumental Analysis*; Thomson: Belmont, CA, 2007; pp 343–346.
- (22) Billo, E. J. *EXCEL for Chemists*; Wiley-VCH: New York, 2001.
- (23) Cubberley, M. S.; Iverson, B. L. *J. Am. Chem. Soc.* **2001**, *123*, 7560.
- (24) Gabriel, G.; Iverson, B. L. *J. Am. Chem. Soc.* **2002**, *124*, 15174.
- (25) Nishigaki, S.; Yoshioka, H.; Nakatsu, K. *Acta Crystallogr.* **1978**, *B34*, 875.
- (26) Hensen, K.; Spangenberg, B.; Bolte, M. *Acta Crystallogr., Sect. C: Cryst. Struct. Commun.* **2000**, *56*, 208.
- (27) Carolan, A. E.; Hancock, R. D., to be published.
- (28) Hancock, R. D. *Acc. Chem. Res.* **1990**, *26*, 875.
- (29) Hancock, R. D. *Prog. Inorg. Chem.* **1989**, *37*, 187.
- (30) *Hyperchem program*, version 8.0; Hypercube, Inc.: Waterloo, Ontario, Canada.
- (31) Allinger, N. L. *J. Am. Chem. Soc.* **1977**, *98*, 8127.
- (32) Martell, A. E.; Smith, R. M. *Critical Stability Constant Database No. 46*; National Institute of Science and Technology (NIST): Gaithersburg, MD, 2003.
- (33) Shannon, R. D. *Acta Crystallogr., Sect. A* **1976**, *A32*, 751.
- (34) Hamilton, J. M.; Anhorn, M. J.; Oscarson, K. A.; Reibenspies, J. H.; Hancock, R. D. *Inorg. Chem.*, in press; ASAP, DOI: 10.1021/ic101742x.
- (35) Shimoni-Livny, L.; Glusker, J. P.; Bock, C. P. *Inorg. Chem.* **1998**, *37*, 1853.
- (36) Hancock, R. D.; Reibenspies, J. H.; Maumela, H. *Inorg. Chem.* **2004**, *43*, 2981.
- (37) Harrowfield, J. M.; Marandi, F.; Soudi, A. A. *Inorg. Chim. Acta* **2005**, *358*, 4099.
- (38) Nash, K. L.; Madic, C.; Mathur, J. N.; Lacquement, J. *The chemistry of the actinide and transactinide elements*, 3rd ed.; Morss, L. R., Edelstein, N. M., Fuger, J., Eds.; Springer: The Netherlands, 2006; Vol. 4, p 2622.
- (39) Kolarik, Z. *Chem. Rev.* **2008**, *108*, 4208.